Mutation in *LBX1/Lbx1* precludes transcription factor cooperativity and causes congenital hypoventilation in humans and mice

Luis Rodrigo Hernandez-Miranda[a], Daniel M. Ibrahim[b,c,1], Pierre-Louis Ruffault[a,d,1], Madeleine Larrosa[a], Kira Balueva[a], Thomas Müller[a], Willemien de Weerd[e], Irene Stolte-Dijkstra[f], Robert M. W. Hostra[f], Jean-François Brunet[g], Gilles Fortin[d], Stefan Mundlos[b,c], and Carmen Birchmeier[a,2]

[a]Developmental Biology and Signal Transduction Group, Max-Delbrueck-Centrum in the Helmholtz Association, 13125 Berlin, Germany; [b]Development and Disease Group, Max Planck Institute for Molecular Genetics, 14195 Berlin, Germany; [c]Institute for Medical and Human Genetics, Charité Universitätsmedizin Berlin, 13353 Berlin, Germany; [d]Hindbrain Integrative Neurobiology Group, Paris-Saclay Institute for Neuroscience, UMR9197/CNRS, 91190 Gif sur Yvette, France; [e]Department of Genetics, University Medical Center Groningen, University of Groningen, 9700 RB Groningen, The Netherlands; [f]Department of Clinical Genetics, Erasmus University Medical Center, 3015 CN Rotterdam, The Netherlands; and [g]Institut de Biologie, École Normale Supérieure, 75005 Paris, France

Edited by Samuel L. Pfaff, The Salk Institute, La Jolla, CA, and accepted by Editorial Board Member Kathryn V. Anderson November 1, 2018 (received for review August 5, 2018)

The respiratory rhythm is generated by the preBötzinger complex in the medulla oblongata, and is modulated by neurons in the retrotrapezoid nucleus (RTN), which are essential for accelerating respiration in response to high CO_2. Here we identify a *LBX1* frameshift (*LBX1*^{FS}) mutation in patients with congenital central hypoventilation. The mutation alters the C-terminal but not the DNA-binding domain of *LBX1*. Mice with the analogous mutation recapitulate the breathing deficits found in humans. Furthermore, the mutation only interferes with a small subset of Lbx1 functions, and in particular with development of RTN neurons that coexpress Lbx1 and Phox2b. Genome-wide analyses in a cell culture model show that Lbx1^{FS} and wild-type Lbx1 proteins are mostly bound to similar sites, but that Lbx1^{FS} is unable to cooperate with Phox2b. Thus, our analyses on Lbx1^{FS} (dys)function reveals an unusual pathomechanism; that is, a mutation that selectively interferes with the ability of Lbx1 to cooperate with Phox2b, and thus impairs the development of a small subpopulation of neurons essential for respiratory control.

congenital hypoventilation | transcriptional cooperativity | *LBX1/Lbx1* | Phox2b | neuronal fate change

Neurons represent the most diverse cell population in animals. How this diversity is specified and maintained is incompletely understood. Available evidence shows that multiple transcription factors cooperate to control common as well as neuron-specific gene expression programs (1, 2). The combinatorial binding of such factors to regulatory elements in chromatin is key for gene expression (3). Homeodomain transcription factors, among them Lbx1 and Phox2b, impose specific neuronal fates during development. In mice, Lbx1 specifies distinct neuronal subtypes in the spinal cord and hindbrain (4–7), and it is also essential for limb muscle development (8–10). Phox2b controls development of central and peripheral visceral neurons (11, 12). In the hindbrain, a single neuronal population (dB2 neurons) coexpresses Lbx1 and Phox2b and depends on both factors for proper development (6, 7, 13). A subpopulation of dB2 neurons forms the retrotrapezoid nucleus (RTN), a small group of cells in the ventral hindbrain that is central for the hypercapnic reflex; that is, the acceleration of breathing in response to increased partial pressure of CO_2 levels (13–16).

Breathing is regulated unconsciously by the nervous system. The respiratory rhythm is generated by the preBötzinger complex located in the ventral hindbrain (17), and is modulated by RTN neurons and by other neuronal populations. Congenital central hypoventilation syndrome (CCHS, also known as Ondine's curse; OMIM 209880) is a rare, life-threatening disorder characterized by slow and shallow breathing resulting from a deficiency in autonomic control of respiration. Patients with CCHS are hypercapnic; that is, they have abnormally high levels of CO_2 in the blood and lack the hypercapnic reflex (18). Atypical heterozygous expansions of alanine repeats in *PHOX2B* are the most common genetic causes of CCHS (12, 19), but similar phenotypes can also be caused by genetic abnormalities in *RET*, *EDN3*, and *MYO1H* (20, 21). The introduction of a frequent *PHOX2B* (*PHOX2B*$^{+27Ala}$) mutation into the murine genome precludes development of RTN neurons, causes loss of the hypercapnic reflex, produces severe hypoventilation, and results in neonatal lethality (13). However, the selective elimination of RTN neurons accounts only for the loss of the hypercapnic reflex, but not for the severe hypoventilation and the neonatal lethality observed in *Phox2b*$^{+27Ala}$ mutant mice (22).

In this study, we report on a consanguineous family with two CCHS-diagnosed children that tested negative for *PHOX2B* mutations. The children carried a homozygous frameshift mutation in *LBX1* (*LBX1*^{FS}) that alters the C terminus of the

Significance

Maintaining low CO_2 levels in our bodies is critical for life and depends on neurons that generate the respiratory rhythm and monitor tissue gas levels. Inadequate response to increasing levels of CO_2 is common in congenital hypoventilation diseases. Here, we identified a mutation in *LBX1*, a homeodomain transcription factor, that causes congenital hypoventilation in humans. The mutation alters the C terminus of the protein without disturbing its DNA-binding domain. Mouse models carrying an analogous mutation recapitulate the disease. The mutation spares most Lbx1 functions, but selectively affects development of a small group of neurons central in respiration. Our work reveals a very unusual pathomechanism, a mutation that hampers a small subset of functions carried out by a transcription factor.

Author contributions: L.R.H.-M., S.M., and C.B. designed research; L.R.H.-M., D.M.I., P.-L.R., M.L., K.B., T.M., W.d.W., I.S.-D., R.M.W.H., and G.F. performed research; J.-F.B. contributed new reagents/analytic tools; L.R.H.-M., G.F., S.M., and C.B. analyzed data; and L.R.H.-M. and C.B. wrote the paper.

The authors declare no conflict of interest.

This article is a PNAS Direct Submission. S.L.P. is a guest editor invited by the Editorial Board.

[1]D.M.I. and P.-L.R. contributed equally to this work.

[2]To whom correspondence should be addressed. Email: cbirch@mdc-berlin.de.

This article contains supporting information online at www.pnas.org/lookup/suppl/doi:10.1073/pnas.1813520115/-/DCSupplemental.

Published online November 28, 2018.

protein without affecting its homeodomain. Homozygous mice carrying the analogous mutation ($Lbx1^{FS/FS}$) displayed respiratory deficits that recapitulated the human phenotype. In $Lbx1^{FS/FS}$ mice, two $Lbx1^{+}$/$Phox2b^{+}$ neuronal subpopulations (in the RTN and in the dorsal hindbrain) were severely affected, but in contrast to *Lbx1* null mutants, second-order somatosensory neurons and limb skeletal muscle formed correctly. Genomewide DNA binding analysis of $Lbx1^{FS}$ in a cell culture model showed that the mutant variant mostly binds to similar sites as the wild-type protein. However, in contrast to the wild-type protein, $Lbx1^{FS}$ is unable to correctly cooperate with Phox2b, and instead overrides its function. Thus, the $Lbx1^{FS}$ protein is selectively impaired in a transcriptional cooperativity with Phox2b during neuronal development, but functions correctly in other contexts.

Results

A Homozygous LBX1 Frameshift Mutation Causes Recessive Congenital Central Hypoventilation Syndrome. We identified two male siblings, offspring from a consanguineous marriage, who displayed hypoventilation during the neonatal period. The parents were unaffected and had a healthy daughter (Fig. 1*A*). Two sisters from the father/mother side of the patients lost a child to cot death (*SI Appendix*, Fig. S1*A*). Both affected siblings studied here required continuous mechanical ventilation after birth because of respiratory insufficiency. They showed recurrent episodes of apnea and signs of central hypoventilation during sleep with no response to falling oxygen saturation or hypercapnia. The children were diagnosed with a severe pattern of classic CCHS. Sanger sequencing, microsatellite analysis, and multiplex ligation-dependent probe amplification of DNA from the children did not reveal any mutations in *PHOX2B*. *Lbx1* ablation causes hypoventilation in newborn mice (6, 7). We therefore sequenced *LBX1* in the affected individuals and identified a homozygous frameshift mutation in its exon 2 ($LBX1^{FS}$ mutation; *SI Appendix*, Fig. S1 *B* and *C*). Sanger sequencing of the entire family confirmed that the $LBX1^{FS}$ mutation segregated with the phenotype. The mutation was predicted to alter the LBX1 protein at the C terminus without affecting its homeodomain (*SI Appendix*, Fig. S1*C*). Furthermore, the $LBX1^{FS}$ variant was absent in control cohorts such as Exome Aggregation Consortium and 1000 Genomes. Ablation of *Lbx1* in mice results in a complex phenotype resulting from defects in the development of various hindbrain neuronal subtypes (dB1–dB4; see scheme in Fig. 1*B*), as well as deficits in the formation of dorsal spinal cord neurons and limb skeletal muscle (4–10, 23). However, the children carrying the $LBX1^{FS/FS}$ mutation did not show any obvious change in limb musculature. We thus reasoned that the $LBX1^{FS/FS}$ mutation might selectively impair neurons that participate in the central control of respiration.

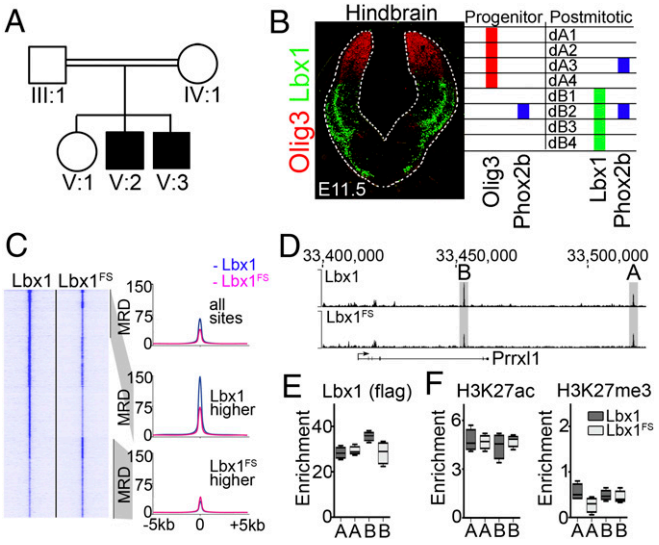

Fig. 1. Genome-wide characterization of chromatin binding of a frameshift mutant LBX1 associated with CCHS in humans. (*A*) Pedigree of a family with two children diagnosed with CCHS (black). (*B*, *Left*) Transverse section of the developing brainstem stained with Olig3 (red) and Lbx1 (green) antibodies at E11.5. Olig3 is expressed in the dorsal brainstem, whereas Lbx1 is expressed in dB1–dB4 neurons. (*B*, *Right*) Scheme showing genes expressed in progenitor cells and neurons of the dorsal hindbrain. Lbx1 and Phox2b are coexpressed in dB2 neurons. (*C*, *Left*) Heat maps showing read tracks at sites occupied by Lbx1 and $Lbx1^{FS}$ ± 5 kb around the binding sites. (*C*, *Right*) Lbx1 (blue) and $Lbx1^{FS}$ (pink) mean read densities (MRDs) for distinct classes of binding sites. (*D*) ChIP-seq tracks illustrating Lbx1 and $Lbx1^{FS}$ occupancy on intergenic and intronic regions of *Prxxl1*. (*E*) ChIP-qPCR analysis using antibodies against flag-tag to validate Lbx1 and $Lbx1^{FS}$ occupancy on the highlighted regions displayed in *D* (n = 4 independent replicates). (*F*) H3K27ac (*Left*) and H3K27me3 (*Right*) ChIP-qPCR analysis performed on chromatin prepared from Lbx1 and $Lbx1^{FS}$ differentiated neurons (n = 4 independent replicates).

Similarities in the Genome-Wide Binding of Lbx1 and $Lbx1^{FS}$. To model alterations of $Lbx1^{FS}$ function and its binding to DNA in a neuronal context, we looked for a suitable neuronal cell culture system. P19 murine embryonic teratocarcinoma stem cells differentiate into neurons that express *Lbx1* and a *HoxA* gene code typical of the caudal hindbrain (rhombomeres 4–7) and anterior cervical spinal cord upon retinoic acid treatment (*SI Appendix*, Fig. S1 *D* and *E*) (24). In addition, they express *Lmx1b*, *Pou4f1*, and *Prrxl1*, the latter at low levels (*SI Appendix*, Fig. S1*F*); this combination is indicative of excitatory somatosensory neurons of the spinal cord and hindbrain. We used this model to analyze Lbx1 and $Lbx1^{FS}$ binding on a genome-wide scale. The endogenous *Lbx1* locus was first mutated in these cells using CRISPR-Cas9, and the resulting *Lbx1* mutant cells were transduced with retroviruses encoding flag-tagged *Lbx1* or $Lbx1^{FS}$ (referred to as Lbx1 and $Lbx1^{FS}$ cells). Cell clones that expressed comparable levels of *Lbx1*/$Lbx1^{FS}$ were chosen for ChIP-seq analysis. In neurons differentiated from such cells (named Lbx1 and $Lbx1^{FS}$ neurons), we identified 7,537 binding sites for Lbx1, but considerably more (n = 12,343) sites for $Lbx1^{FS}$. A large fraction (59%) of the Lbx1 sites was also bound by $Lbx1^{FS}$ (*SI Appendix*, Fig. S1*G*). To analyze how the 1.6-fold increase in $Lbx1^{FS}$ binding sites related to binding strength, another important variable for transcription factor function, we performed read enrichment analysis combined with *k*-means clustering for Lbx1- and $Lbx1^{FS}$-bound sites. In general, the mean read density for $Lbx1^{FS}$ was lower than for Lbx1 (Fig. 1*C*). Sites in which $Lbx1^{FS}$ bound more strongly than Lbx1 displayed, on average, low enrichment for both $Lbx1^{FS}$ and Lbx1 proteins (Fig. 1*C*). Together, our data show that the $Lbx1^{FS}$ mutant protein can bind to most Lbx1 sites; however, the binding is weaker and less specific than that of the wild-type protein.

Inspection of Lbx1 and $Lbx1^{FS}$ ChIP-seq tracks revealed occupancy of both factors on intronic and intergenic regions associated with the somatosensory genes *Prrxl1*, *Lmx1b*, and *Pou4f1* (Fig. 1*D* and *SI Appendix*, Fig. S2*A*). The occupancy of Lbx1/$Lbx1^{FS}$ on such loci was confirmed by ChIP-qPCR (Fig. 1*E* and *SI Appendix*, Fig. S2*B*). Similar gene expression levels for the three somatosensory genes were observed in neurons differentiated from Lbx1 and $Lbx1^{FS}$ cells, but they were not expressed in *Lbx1* mutant neurons (*SI Appendix*, Fig. S2*C*). To test whether these intronic and intergenic regions correspond to enhancer elements, we performed ChIP-qPCR for H3K27ac and H3K27me3, two epigenetic marks associated with active or repressed enhancers, respectively (25). This showed strong enrichment for H3K27ac at the analyzed loci in neurons differentiated from Lbx1 and $Lbx1^{FS}$ cells, whereas H3K27me3 was not enriched (Fig. 1*F* and *SI Appendix*, Fig. S2*D*). Hence, Lbx1/$Lbx1^{FS}$ binding sites on the *Lmx1b*,

Prrxl1, and *Pou4f1* loci correspond to active enhancers in Lbx1 and Lbx1^{FS} neurons.

We next performed de novo motif analysis for Lbx1 and Lbx1^{FS} binding sites. In both peak sets, various AT-rich motifs that aligned with previously identified Lbx1-binding sites were overrepresented (26). A closer inspection revealed subtle differences between Lbx1 and Lbx1^{FS} sequence preferences (*SI Appendix*, Fig. S3). The most significantly enriched motif in Lbx1^{FS} peaks was a nonpalindromic 8-mer, possibly representing a monomer-binding site, which was identified in Lbx1 sites as the fifth most significant. In contrast, the most overrepresented motif in Lbx1 sites was a 12-mer palindrome, possibly a homodimeric site that was the third-most enriched motif for Lbx1^{FS}. Finally, a 16-bp-long nonpalindromic motif was identified in Lbx1, but not Lbx1^{FS}, sites (*SI Appendix*, Fig. S3*A*). This was composed of a partial Lbx1 site at the 3′ end, preceded with a distinct AT-rich 5′ sequence, which could represent the binding site of an Lbx1 cofactor. Interestingly, this AT-rich half-site was reported to be a preferred Phox2b binding site (*SI Appendix*, Fig. S3*B*) (27). This raised the possibility that although the general DNA binding of Lbx1^{FS} was only mildly compromised, its ability to interact with other factors is more severely impaired.

Hypoventilation and Lack of Hypercapnic Reflex in Homozygous *Lbx1$^{FS/FS}$* Mice. To better understand the deficit in LBX1^{FS} function, we introduced an analogous mutation into the mouse *Lbx1* gene (*SI Appendix*, Fig. S4*A*). Heterozygous *Lbx1^{FS}* (*Lbx1$^{FS/+}$*) mice were viable and fertile, and did not show an obvious phenotype. However, homozygous *Lbx1$^{FS/FS}$* newborn mice displayed cyanosis and died (n = 18/18) within the first 2 h of life without displaying other apparent deficits in motor behavior. Plethysmographic recordings revealed pronounced respiratory deficits in *Lbx1$^{FS/FS}$* mice; that is, shallow breathing with frequent and long apneas (Fig. 2*A* and *SI Appendix*, Fig. S5*A*). In particular, *Lbx1$^{FS/FS}$* mice displayed longer times between breathing cycles (T_{tot}), which led to reduced respiratory minute volumes (V_E) and severe hypoventilation (Fig. 2 *A* and *B* and *SI Appendix*, Fig. S5 *A–C*). Importantly, *Lbx1$^{FS/FS}$* mice lacked the hypercapnic reflex and did not change ventilation (V_E and T_{tot}) when exposed to high levels of CO_2 in air (Fig. 2 *A* and *B* and *SI Appendix*, Fig. S5 *A–C*). We concluded that the *Lbx1$^{FS/FS}$* mutation in mice leads to a respiratory phenotype that resembles the one observed in the studied patients.

The *Lbx1$^{FS/FS}$* Mutation Interferes with RTN Formation. We next assessed whether the lack of hypercapnic response in *Lbx1$^{FS/FS}$* mice was a result of impaired RTN development. RTN neurons locate in the ventral hindbrain and coexpress Lbx1 and Phox2b, but not choline acetyl-transferase (ChAT) (Lbx1$^+$/Phox2b$^+$/ChAT$^-$), and are thus distinguished from the neighboring facial motor neurons that coexpress Phox2b and ChAT, but not Lbx1 (Lbx1$^-$/Phox2b$^+$/ChAT$^+$). In *Lbx1$^{FS/FS}$* animals, Phox2b$^+$/Lbx1$^+$ cells were absent in the RTN region either at embryonic day (E) 14.5 or at birth (Fig. 2*C*). However, several other Lbx1$^+$ neuronal types were present and expressed Lbx1 at apparently normal levels. The absence of a functional RTN was confirmed by Ca^{2+} imaging (*SI Appendix*, Fig. S5 *D* and *E*). Further analyses demonstrated that RTN precursors (i.e., Lbx1$^+$/Phox2b$^+$ dB2 neurons) were unchanged in *Lbx1$^{FS/FS}$* mice at E11.5, but failed to initiate *Atoh1* expression during their migration toward the ventral hindbrain at E12.5 (*SI Appendix*, Fig. S5 *F–H*). preBötzinger complex neurons have no history of Phox2b or Lbx1 expression (28), and were present and functional in *Lbx1$^{FS/FS}$* mice (*SI Appendix*, Fig. S5*I*). We conclude that in *Lbx1$^{FS/FS}$* mice, dB2 neuronal precursors are correctly specified, but the subset destined to form the RTN fails to express *Atoh1* and does not migrate into the position where the RTN normally resides.

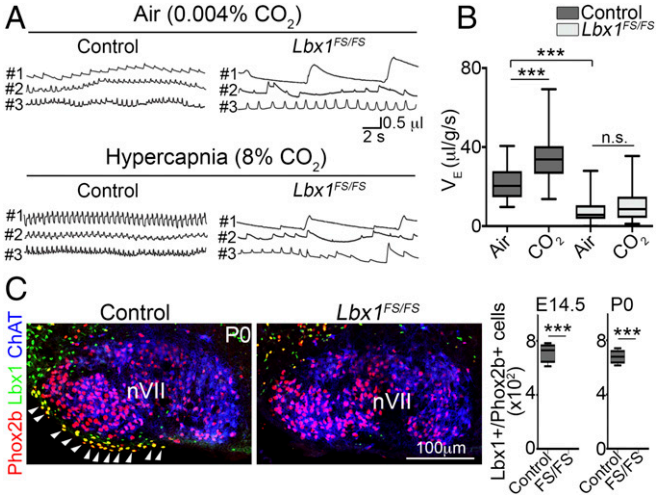

Fig. 2. The *Lbx1^{FS}* mutation causes central hypoventilation and loss of CO_2 sensitivity in mice. (*A*) Plethysmographic traces of control and *Lbx1$^{FS/FS}$* mice in normal air (0.04% CO_2; *Top* traces) and high CO_2-containing air (hypercapnia, 8% CO_2, *Bottom* traces). Numbers on the left of the traces indicate distinct individuals. (*B*) Quantification of V_E of control (n = 9) and *Lbx1$^{FS/FS}$* (n = 10) newborn mice in normal air and high CO_2-containing air (unpaired nonparametric Mann–Whitney U test). (*C*, *Left* and *Middle*) Histological analysis of RTN neurons (arrowheads) using Lbx1 (green) and Phox2b (red) antibodies; these neurons are present in control mice but not in *Lbx1$^{FS/FS}$* mice at birth. Antibodies against ChAT (blue) were used to distinguish RTN (Lbx1$^+$/Phox2b$^+$/ChAT$^-$) neurons from facial (nVII) motor (Lbx1$^-$/Phox2b$^+$/ChAT$^+$) neurons. Confocal tile scan modus was used to acquire photomicrographs and assembled using ZEN2012 software (10% overlap between tiles). (*C*, *Right*) Quantification of RTN neuron numbers in control and *Lbx1$^{FS/FS}$* mice at E14.5 (n = 4 per condition; unpaired t test, t = 19,37; df = 6) and at birth (n = 4 per condition; unpaired t test, t = 26,08; df = 6). ***$P < 0.0001$.

The *Lbx1$^{FS/FS}$* Mutation Does Not Preclude SpV and Limb Muscle Development. Next we analyzed inhibitory and excitatory somatosensory neurons of the spinal trigeminal (SpV) nucleus. These neurons are absent in *Lbx1* null mutant mice, where they instead assumed solitary tract nucleus and inferior olivary nucleus neuronal fates, respectively (7). Interestingly, the SpV was present in *Lbx1$^{FS/FS}$* mice (Fig. 3*A*). Furthermore, the solitary tract and inferior olivary nuclei appeared to have a normal size (Fig. 3*A*). Finally, limb muscle development is severely affected in *Lbx1* null mutant mice (8–10), but these muscle groups were present and appeared correctly formed in *Lbx1$^{FS/FS}$* mice (Fig. 3*B*). Together, our analyses demonstrate that the *Lbx1^{FS}* mutation selectively interferes with development of Lbx1$^+$/Phox2b$^+$ RTN neurons, but in other contexts, the mutant protein functions correctly, as in development of somatosensory SpV neurons and limb muscles.

dB2 Neurons Are Responsible for the Breathing Deficits Observed in *Lbx1$^{FS/FS}$* Mice. To assess whether the breathing deficits observed in *Lbx1$^{FS/FS}$* mice exclusively depend on dysfunction of dB2 derivatives, we conditionally restricted the *Lbx1^{FS}* mutation to the dB2 lineage by using *Phox2b^{cre}* (*Phox2b$^{cre/+}$;Lbx1$^{FS/lox}$*, named *dB2-Lbx1^{FS}* mice; see *SI Appendix*, Fig. S6*A* for a scheme of the strategy). In such animals, neurons with a history of *Phox2b* expression carried an *Lbx1$^{\Delta/FS}$* genotype, but other cells (*Lbx1$^{FS/lox}$*) retained one copy of a fully functional *Lbx1^{lox}* allele (*SI Appendix*, Fig. S4*B*). In *dB2-Lbx1^{FS}* animals, RTN neurons were absent (Fig. 4*A*). Plethysmographic recordings of *dB2-Lbx1^{FS}* animals showed a full recapitulation of the physiological phenotype observed in *Lbx1$^{FS/FS}$* animals (i.e., severe hypoventilation, lack of the hypercapnic reflex, frequent apneas; *SI Appendix*, Fig. S6 *C–G*;

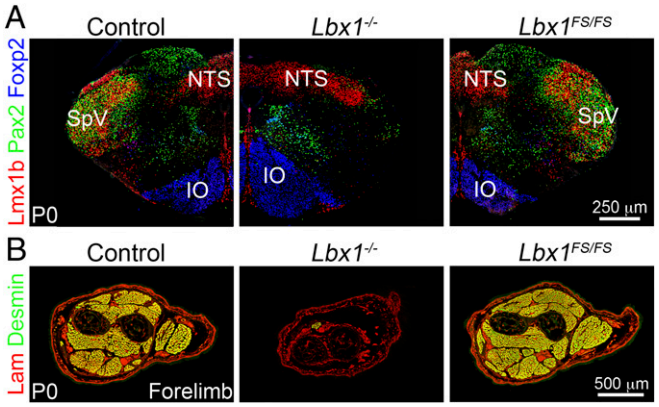

Fig. 3. Development of somatosensory neurons and limb muscle in *Lbx1*$^{FS/FS}$ mice. (*A*) Histological analysis of somatosensory neurons of the SpV, viscerosensory neurons of the nucleus of the solitary tract (NTS), and neurons of the inferior olive (IO) in control (*Left*), *Lbx1* null (*Lbx1*$^{-/-}$; *Middle*), and *Lbx1*$^{FS/FS}$ (*Right*) mutant newborn mice. Pax2 (green) and Lmx1b (red) antibodies distinguish inhibitory and excitatory somatosensory neurons of the spinal trigeminal nucleus, respectively. NTS neurons express Lmx1b, and inferior olivary neurons express Foxp2 (blue). (*B*) Histological analysis of limb muscles in control, *Lbx1*$^{-/-}$, and *Lbx1*$^{FS/FS}$ newborn mice, using antibodies against laminin (Lam, red) and desmin (green). Confocal tile scan modus was used to acquire photomicrographs, and assembled using ZEN2012 software (10% overlap between tiles). Photomicrographs were mounted on a black frame to maintain figure panel proportions.

summarized in Fig. 4*B*), as well as lethality (n = 12/12) within the first 2 h of life. Thus, all respiratory deficits associated with the *Lbx1*^{FS} mutation are the result of a selective developmental deficit in the dB2 neuronal lineage.

RTN neurons arise from rhombomere 5 (29). We next restricted the *Lbx1*^{FS} mutation to rhombomeres 3 and 5, using *Egr2*^{cre} that only recombines cells in these rhombomeres (*Egr2*$^{cre/+}$;*Lbx1*$^{FS/lox}$, named *Egr2-Lbx1*^{FS} mice; see *SI Appendix*, Fig. S6*B* for a scheme of the strategy). As expected, RTN neurons were absent in *Egr2-Lbx1*^{FS} animals (Fig. 4*A*). Plethysmographic recordings of *Egr2-Lbx1*^{FS} mice showed that they were unable to respond to high CO_2 levels in the air (*SI Appendix*, Fig. S6 *C–G*). Nevertheless, *Egr2-Lbx1*^{FS} mice did not display apneas and survived the postnatal period (n = 11/11), with a mild hypoventilation that was observed in their early postnatal life (*SI Appendix*, Fig. S6 *D* and *H*). The response of *Egr2-Lbx1*^{FS} mice to high levels of CO_2 improved with maturation, but even adult mutants presented a blunted hypercapnic reflex (*SI Appendix*, Fig. S6*H*). This phenotype, largely similar to the one observed after conditional mutation of *Phox2b*$^{+27ala}$ in rhombomeres 3 and 5 (22), implies that several neuronal groups originating from dB2 precursors participate in the control of breathing.

We next used intersectional lineage tracing to specifically label dB2 derivatives with Tomato fluorescent protein, using *Lbx1*$^{cre/+}$;*Phox2b*$^{Flpo/+}$;*Ai65*$^{ds/+}$ animals (see *SI Appendix*, Fig. S7*A* for a scheme of the strategy). Tomato$^+$/Lbx1$^+$/Phox2b$^+$ cells were found, in addition to the RTN, around the trigeminal motor nucleus in rhombomere 1 and 2 (a population known as periV neurons), as well as in the dorsal part of rhombomeres 3–6 (*SI Appendix*, Fig. S7 *B–D*). We compared development of these two dB2 derivatives (periV neurons and neurons in the dorsal part of the hindbrain) in strains displaying the most severe breathing phenotype (i.e., *Lbx1*$^{FS/FS}$, *dB2-Lbx1*^{FS}) and the milder breathing deficit (*Egr2-Lbx1*^{FS}). Lbx1$^+$/Phox2b$^+$ periV neurons were present in normal numbers in all analyzed strains (quantified in Fig. 4*B*). However, the number of dorsally located Lbx1$^+$/Phox2b$^+$ neurons was severely reduced in *Lbx1*$^{FS/FS}$ and *dB2-Lbx1*^{FS} animals, but not obviously affected in *Egr2-Lbx1*^{FS} mice (Fig. 4*B* and *SI Appendix*, Fig. S7*E*). Thus, the absence of the RTN combined with the reduction of the dorsal Lbx1$^+$/Phox2b$^+$ population correlates with the severe breathing phenotype observed in *Lbx1*$^{FS/FS}$ and *dB2-Lbx1*^{FS} mutants.

Ectopic Expression of Somatosensory Genes in *Lbx1*^{FS}*/Phox2b* Expressing Neurons. To assess whether the absent dB2 neurons in *Lbx1*$^{FS/FS}$ mice assumed an aberrant neuronal fate, we extended our intersectional genetic lineage tracing to *Lbx1*^{FS} (*Lbx1*$^{cre/FS}$;*Phox2b*$^{Flpo/+}$;*Ai65*$^{dss/+}$; see *SI Appendix*, Fig. S7*A*) mutant mice. This demonstrated that ectopic Tomato$^+$ cells appeared in the somatosensory SpV nucleus of *Lbx1*^{FS} mice, which were not observable in control animals (Fig. 5*A* and *SI Appendix*, Fig. S8*A*). These ectopic Tomato$^+$ cells coexpressed markers of excitatory somatosensory neurons such as Prrxl1 or Lmx1b (Fig. 5 *A* and *B* and *SI Appendix*, Fig. S8*B*). Thus, the *Lbx1*^{FS} mutation selectively affects the development of an Lbx1$^+$/Phox2b$^+$ dB2 subpopulation that adopts an aberrant somatosensory fate.

We next modeled the (dys)function of Lbx1^{FS} in Phox2b$^+$ neurons, using our cell culture model. For this, *Lbx1* mutant P19 cells were transduced with retroviruses encoding a HA-tagged version of Phox2b (hereafter Phox2b cells) alone or in combination with flag-tagged Lbx1 or Lbx1^{FS} (Lbx1/Phox2b and Lbx1^{FS}/Phox2b cells). We then sequenced the transcriptomes of neurons differentiated from these cells. Hierarchical expression clustering showed that Phox2b, Lbx1/Phox2b, and Lbx1^{FS}/Phox2b neurons were clearly distinct from Lbx1 neurons and clustered separately (Fig. 5*C*). Nevertheless, Lbx1 and Lbx1^{FS}/Phox2b neurons were more closely related to each other than to Lbx1/Phox2b or Phox2b neurons (Fig. 5*C*). Interestingly, the *Prrxl1*, *Lmx1b*, and *Pou4f1* somatosensory genes were among the

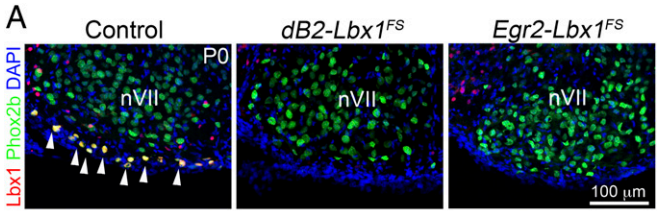

B

dB2 neuronal population	Control (# cells)	*Lbx1*$^{FS/FS}$ (# cells)	*dB2-Lbx1*^{FS} (# cells)	*Egr2-Lbx1*^{FS} (# cells)
RTN (r5/6)	732 +/- 20	0 (p<0.0001)	0 (p<0.0001)	0 (p<0.0001)
Dorsal (r3-r6)	2875 +/- 85	636 +/- 36 (p<0.0001)	649+/-30 (p<0.0001)	2898 +/- 74 (p=0.95)
PeriV (r1/r2)	1903 +/- 61	1932 +/- 61 (p=0.92)	1954 +/- 45 (p=0.92)	1922 +/- 49 (p=0.92)

Ventilation	Control	*Lbx1*$^{FS/FS}$	*dB2-Lbx1*^{FS}	*Egr2-Lbx1*^{FS}
Air (μl/g/s)	27.1 +/- 0.25	11.2 +/- 0.26 (p<0.0001)	15.2 +/- 0.36 (p<0.0001)	22.3 +/- 0.46 (p<0.0001)
Hypercapnia (μl/g/s)	39.5 +/- 0.52	10.4 +/- 0.57 (p<0.0001)	17.1 +/- 0.24 (p<0.0001)	19.7 +/- 0.39 (p<0.0001)

Fig. 4. Conditional mutagenesis restricts the *Lbx1*^{FS} mutation to specific neuronal subpopulations. (*A*) Analysis of Lbx1$^+$ (red) Phox2b$^+$ (green) RTN neurons (arrowheads) in control, *dB2-Lbx1*^{FS} and *Egr2-Lbx1*^{FS} newborn mice. DAPI (blue) was used as a counterstain, and the facial (nVII) motor nucleus is indicated. Confocal tile scan modus was used to acquire photomicrographs, and assembled using ZEN2012 software (10% overlap between tiles). (*B*, *Top*) Comparison of dB2 neuron numbers: RTN neurons [one-way ANOVA, F (3, 15) = 883.4]; dorsal Lbx1$^+$/Phox2b$^+$ neurons [one-way ANOVA, F(3, 15) = 370] and periV neurons [one-way ANOVA, F(3, 15) = 0.1562] in control (n = 6) *Lbx1*$^{FS/FS}$ (n = 4), *Egr2-Lbx1*^{FS} (n = 4), and *dB2-Lbx1*^{FS} (n = 4) mice. (*B*, *Bottom*) Comparison of ventilatory minute volumes in normal air and in hypercapnia in control (n = 20) *Lbx1*$^{FS/FS}$ (n = 11), *Egr2-Lbx1*^{FS} (n = 11), and *dB2-Lbx1*^{FS} (n = 12) mice (unpaired nonparametric Mann–Whitney U test).

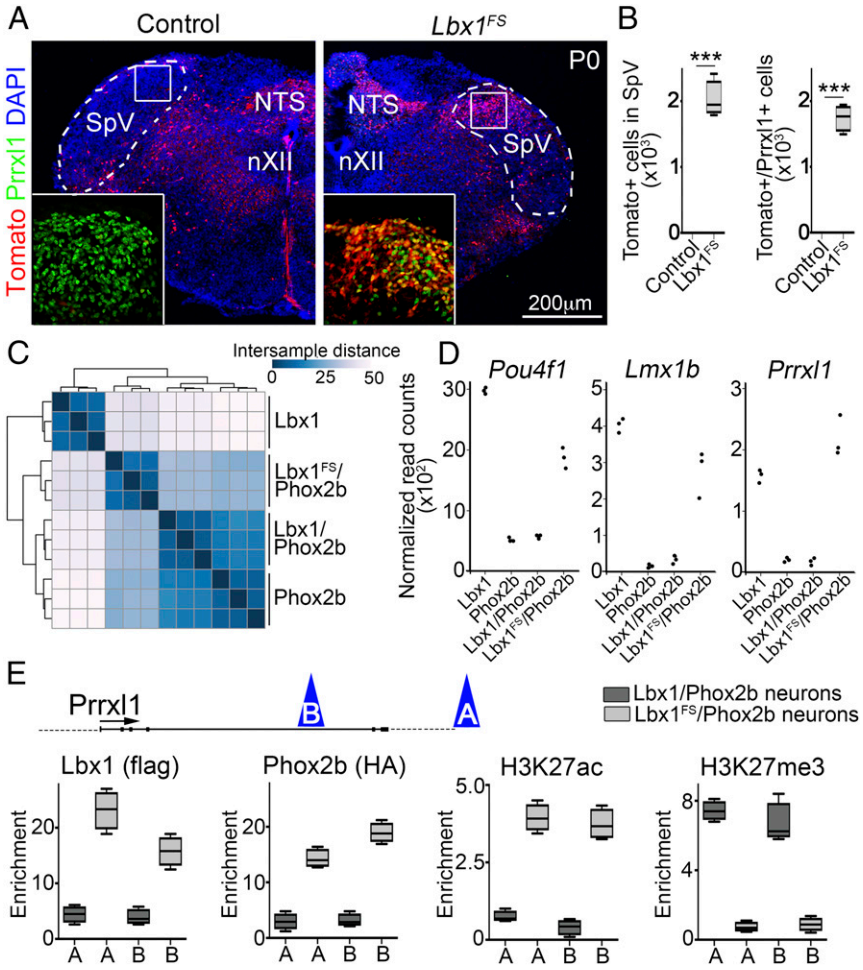

Fig. 5. Mis-specification of dB2 neurons in *Lbx1*^{FS} mice. (*A* and *B*) Intersectional labeling of dB2 neurons in control (*Lbx1*$^{cre/+}$;*Phox2b*$^{Flpo/+}$;*Ai65*$^{+/-}$) and *Lbx1*^{FS} (*Lbx1*$^{cre/FS}$;*Phox2b*$^{Flpo/+}$;*Ai65*$^{+/-}$) newborn mice (*SI Appendix*, Fig. S6*A*). (*A*) Histological analysis of dB2-Tomato^{+} (red) neurons located in the dorsal part of the SpV nucleus in control and *Lbx1*^{FS} newborn mice. DAPI (blue) was used to counterstain. *Insets* are magnifications (300×) of the boxed areas stained with the somatosensory specific Prxxl1 (green) and Tomato (red) antibodies. Confocal tile scan modus was used to acquire photomicrographs and was assembled using ZEN2012 software (10% overlap between tiles). (*B*) Quantification of Tomato^{+} and Tomato^{+}/Prrxl1^{+} neurons in control and *Lbx1*^{FS} mice at birth ($n = 4$ per genotype; unpaired t test, $t = 17.03$; df = 6). (*C*) Hierarchical transcriptome clustering of Lbx1-, Phox2b-, Lbx1/Phox2b-, and Lbx1^{FS}/Phox2b-expressing neurons ($n = 3$ independent replicates). Color code represents intersample distances (in reads per kilobase per million mapped reads). (*D*) Normalized read counts for *Pou4f1*, *Lmx1b*, and *Prrxl1* transcripts in neurons expressing Lbx1, Phox2b, Lbx1/Phox2b, and Lbx1^{FS}/Phox2b ($n = 3$ independent replicates). (*E*) ChIP-qPCR analysis performed on chromatin prepared from Lbx1/Phox2b and Lbx1^{FS}/Phox2b expressing neurons using antibodies against flag-tag (for Lbx1 and Lbx1^{FS} immunoprecipitation), HA-tag (for Phox2b immunoprecipitation), H3K27ac and, H3K27me3 ($n = 4$ independent replicates). Analyzed sites in the *Prrxl1* locus are indicated schematically as blue triangles (Fig. 1*D*). ***$P < 0.0001$.

most significant and differentially expressed genes in Lbx1^{FS}/Phox2b^{+} neurons compared with Phox2b or Lbx1/Phox2b^{+} neurons (Fig. 5*D*). Thus, Phox2b represses these somatosensory genes alone or even when Lbx1 is present, but this does not occur when Lbx1^{FS} and Phox2b are coexpressed, a change reminiscent of the one observed in vivo where Lbx1^{FS+}/Phox2b^{+} (dB2) neurons assumed an aberrant somatosensory fate.

Next we analyzed chromatin modifications of the previously characterized enhancers of *Prrxl1*, *Lmx1b*, and *Pou4f1* somatosensory genes. In Lbx1/Phox2b neurons, ChIP-qPCR showed a modest enrichment of Lbx1 and Phox2b at the analyzed loci (Fig. 5*E* and *SI Appendix*, Fig. S9). Moreover, the chromatin mark H3K27me3 was enriched in those sites, demonstrating that the enhancers are repressed. However, when the chromatin of Lbx1^{FS}/Phox2b neurons was used for ChIP-qPCR experiments, Lbx1, Phox2b, and H3K27ac were significantly enriched at the *Prrxl1*, *Lmx1b*, and *Pou4f1* enhancers (Fig. 5*E* and *SI Appendix*, Fig. S9). Thus, enhancer sequences of the *Prrxl1*, *Lmx1b*, and *Pou4f1* genes are activated when Lbx1^{FS} and Phox2b are recruited to these sites, but repressed when Lbx1 and Phox2b are recruited.

Discussion

Respiratory disorders in humans range from irregular and unstable respiration to the complete loss of breathing control. The most common causes of congenital hypoventilation are dominant mutations in *PHOX2B* that affect the formation of the RTN. Here we show that a homozygous frameshift mutation in *LBX1* causes severe congenital hypoventilation that resembles classical CCHS. We used cell culture and mouse models to investigate the (dys)function caused by the frameshift mutation, which alters the C-terminal sequence of the protein but spares its homeodomain. In most developmental contexts, the mutant protein exerts its role correctly; that is, the mutation only interferes with small subsets of Lbx1 functions. Our analysis has thus revealed a very unusual pathomechanism of a transcription factor mutation that results in a severe respiratory disorder.

Lbx1^{FS} Protein Correctly Functions in Most Developmental Contexts. Our cell culture modeling of Lbx1^{FS} binding showed that Lbx1^{FS} and Lbx1 largely bind to similar sites genome-wide, which is in agreement with conserved functionality of the Lbx1^{FS} protein in most developmental contexts. Motif analyses revealed subtle differences between the binding preferences of Lbx1 and Lbx1^{FS}. In particular, a specific motif was present in Lbx1, but not in Lbx1^{FS} binding sites, which consists of a 16-bp-long nonpalindromic sequence that is composed of an Lbx1-monodimer site combined with a half-site of another factor. Interestingly, the sequence that represents the second half-site corresponds to the preferred binding motif previously identified for Phox2b (27). This observation suggested a failure of Lbx1^{FS} to cooperate productively with Phox2b.

Lbx1 and Phox2b are known to functionally repress each other: When Lbx1 is mutated, supernumerary Phox2b visceral sensory neurons arise (7). Vice versa, mutation of Phox2b results in the appearance of supernumerary somatosensory Lbx1 neurons (30). Remarkably, development of the dB2 lineage depends on both Lbx1 and Phox2b and relies on the repression of

the somatosensory genes (7, 13). Lbx1-dependent differentiation of somatosensory neurons can be modeled in vitro and occurs in the presence of Lbx1 and Lbx1^{FS}. Interestingly, coexpression of Phox2b represses somatosensory genes in Lbx1^{+} but not Lbx1^{FS+} neurons. In the presence of Phox2b, the altered C-terminal sequence of Lbx1^{FS} might impede the correct recruitment of coregulatory factors, thus accounting for the fact that Lbx1^{FS} is unable to correctly cooperate with Phox2b.

LBX1/Lbx1 in CCHS. Here we demonstrate that the hypomorphic *Lbx1^{FS}* mutation selectively interferes with the development of specific dB2 neuronal populations. Physiologically, *Lbx1$^{FS/FS}$* mice display a plethora of respiratory deficits: slow and irregular breathing, lack of hypercapnic reflex, and frequent and prolonged apneas. Together, these deficits appear to result in neonatal lethality. We observed that the conditional restriction of the *Lbx1^{FS}* mutation to the dB2 lineage (*dB2-Lbx1^{FS}* mice) fully recapitulates the physiological phenotypes observed in *Lbx1$^{FS/FS}$* mice. In contrast, the conditional restriction of the *Lbx1^{FS}* mutation to rhombomeres 3 and 5 (*Egr2-Lbx1^{FS}* mice) impaired RTN neuron development, abolished the hypercapnic reflex, and caused mild hypoventilation, but not abnormal apneas or neonatal mortality. Interestingly, similar or even identical phenotypes are observed when the *Phox2b^{+27ala}* mutation is restricted to rhombomeres 3 and 5 (22). Thus, the *Lbx1^{FS}* mutation causes respiratory deficits that are in part, but not completely, a result of the loss of RTN neurons.

Last, we report in this study that dB2 precursors produce, in addition to the RTN and periV cells, an additional not previously described group of Lbx1^{+}/Phox2b^{+} neurons that locate dorsally in rhombomeres 3–6. Because of the complexity of the developmental deficits displayed by Lbx1 null mutant mice, the contribution of individual cell populations to respiratory deficits had previously not been assessable. We used here intersectional genetic strategies to show that the combined deficits in development of RTN and the dorsal Lbx1^{+}/Phox2^{+} population correlated with severe hypoventilation and neonatal lethality. Further studies will be needed to define the connectivity and the exact function of this dorsal neuronal population.

Materials and Methods

Research Involving Humans and Mice. Venous blood and genomic DNA samples from humans were obtained by standard procedures. Written informed consent was obtained from all individuals. Experimental procedures and animal handling were conducted according to institutional protocols and guidance approved by the Max Delbrueck Center (Berlin), CNRS (Gif sur Yvette), Max Planck Institute for Genetics (Berlin), and the Ethic Committee of the Charité Universitätsmedizin (Berlin). Details on mouse strains are provided in *SI Appendix, SI Materials and Methods*.

Histology. Development of dB2 neuronal derivatives was assessed on 20-μm transverse hindbrain sections from control and mutant mice. Details on antibodies and in situ probes used in this study are provided in *SI Appendix, SI Materials and Methods*.

Cell Cultures. P19 embryonic teratocarcinoma cells were obtained from ATTC (CRL-1825) and differentiated into neurons using 1 μM retinoic acid (Sigma), as described (31). Details on CRISPR-CAS9 mutation of *Lbx1* in P19 cells, retroviral infection, ChIP, and deep sequencing experiments are provided in *SI Appendix, SI Materials and Methods*.

Physiology. Unrestrained plethysmographic recordings of individual mouse pups were carried out as described (32). Further details on plethysmographic recordings and Ca^{2+} imaging studies can be found in *SI Appendix, SI Materials and Methods*.

ACKNOWLEDGMENTS. We thank Christo Goridis (Institut de Biologie, École Normale Supérieure) and Elijah Lowenstein (Max Delbrueck Center) for a critical reading of the manuscript, and Sven Buchert, Petra Stallerow, Claudia Päseler, and Sandra Autran for technical support. Funding for this work was provided by the European Commission (Marie Curie Fellowship 302477 to L.R.H.-M.), Deutsche Forschungsgemeinschaft (SFB 665), Excellence cluster NeuroCure and Helmholtz Association (C.B.), Agence Nationale pour la Recherche (ANR-15-CE16-0013-02 to J.-F.B. and G.F.), European Molecular Biology Organization (long-term fellowship 408-2016 to P.-L.R.), and Fondation pour la Recherche Médicale (DEQ20120323709 to G.F.).

1. Hobert O (2008) Regulatory logic of neuronal diversity: Terminal selector genes and selector motifs. *Proc Natl Acad Sci USA* 105:20067–20071.
2. Lee TI, Johnstone SE, Young RA (2006) Chromatin immunoprecipitation and microarray-based analysis of protein location. *Nat Protoc* 1:729–748.
3. Spitz F, Furlong EE (2012) Transcription factors: From enhancer binding to developmental control. *Nat Rev Genet* 13:613–626.
4. Gross MK, Dottori M, Goulding M (2002) Lbx1 specifies somatosensory association interneurons in the dorsal spinal cord. *Neuron* 34:535–549.
5. Müller T, et al. (2002) The homeodomain factor lbx1 distinguishes two major programs of neuronal differentiation in the dorsal spinal cord. *Neuron* 34:551–562.
6. Pagliardini S, et al. (2008) Central respiratory rhythmogenesis is abnormal in lbx1-deficient mice. *J Neurosci* 28:11030–11041.
7. Sieber MA, et al. (2007) Lbx1 acts as a selector gene in the fate determination of somatosensory and viscerosensory relay neurons in the hindbrain. *J Neurosci* 27:4902–4909.
8. Brohmann H, Jagla K, Birchmeier C (2000) The role of Lbx1 in migration of muscle precursor cells. *Development* 127:437–445.
9. Gross MK, et al. (2000) Lbx1 is required for muscle precursor migration along a lateral pathway into the limb. *Development* 127:413–424.
10. Schäfer K, Braun T (1999) Early specification of limb muscle precursor cells by the homeobox gene Lbx1h. *Nat Genet* 23:213–216.
11. Brunet JF, Pattyn A (2002) Phox2 genes–From patterning to connectivity. *Curr Opin Genet Dev* 12:435–440.
12. Goridis C, Dubreuil V, Thoby-Brisson M, Fortin G, Brunet JF (2010) Phox2b, congenital central hypoventilation syndrome and the control of respiration. *Semin Cell Dev Biol* 21:814–822.
13. Dubreuil V, et al. (2008) A human mutation in Phox2b causes lack of CO2 chemosensitivity, fatal central apnea, and specific loss of parafacial neurons. *Proc Natl Acad Sci USA* 105:1067–1072.
14. Dubreuil V, et al. (2009) Defective respiratory rhythmogenesis and loss of central chemosensitivity in Phox2b mutants targeting retrotrapezoid nucleus neurons. *J Neurosci* 29:14836–14846.
15. Guyenet PG, Abbott SB, Stornetta RL (2013) The respiratory chemoreception conundrum: Light at the end of the tunnel? *Brain Res* 1511:126–137.
16. Ruffault PL, et al. (2015) The retrotrapezoid nucleus neurons expressing Atoh1 and Phox2b are essential for the respiratory response to CO_2. *eLife* 4:e07051.
17. Rekling JC, Feldman JL (1998) PreBötzinger complex and pacemaker neurons: Hypothesized site and kernel for respiratory rhythm generation. *Annu Rev Physiol* 60:385–405.
18. Weese-Mayer DE, Berry-Kravis EM, Ceccherini I, Rand CM (2008) Congenital central hypoventilation syndrome (CCHS) and sudden infant death syndrome (SIDS): Kindred disorders of autonomic regulation. *Respir Physiol Neurobiol* 164:38–48.
19. Amiel J, et al. (2003) Polyalanine expansion and frameshift mutations of the paired-like homeobox gene PHOX2B in congenital central hypoventilation syndrome. *Nat Genet* 33:459–461.
20. Rand CM, Carroll MS, Weese-Mayer DE (2014) Congenital central hypoventilation syndrome: A neurocristopathy with disordered respiratory control and autonomic regulation. *Clin Chest Med* 35:535–545.
21. Spielmann M, et al. (2017) Mutations in *MYO1H* cause a recessive form of central hypoventilation with autonomic dysfunction. *J Med Genet* 54:754–761.
22. Ramanantsoa N, et al. (2011) Breathing without CO(2) chemosensitivity in conditional Phox2b mutants. *J Neurosci* 31:12880–12888.
23. Hernandez-Miranda LR, Müller T, Birchmeier C (2017) The dorsal spinal cord and hindbrain: From developmental mechanisms to functional circuits. *Dev Biol* 432:34–42.
24. Philippidou P, Dasen JS (2013) Hox genes: Choreographers in neural development, architects of circuit organization. *Neuron* 80:12–34.
25. Shlyueva D, Stampfel G, Stark A (2014) Transcriptional enhancers: From properties to genome-wide predictions. *Nat Rev Genet* 15:272–286.
26. Weirauch MT, et al. (2014) Determination and inference of eukaryotic transcription factor sequence specificity. *Cell* 158:1431–1443.
27. Berger MF, et al. (2008) Variation in homeodomain DNA binding revealed by high-resolution analysis of sequence preferences. *Cell* 133:1266–1276.
28. Bouvier J, et al. (2010) Hindbrain interneurons and axon guidance signaling critical for breathing. *Nat Neurosci* 13:1066–1074.
29. Thoby-Brisson M, et al. (2009) Genetic identification of an embryonic parafacial oscillator coupling to the preBötzinger complex. *Nat Neurosci* 12:1028–1035.
30. D'Autréaux F, Coppola E, Hirsch MR, Birchmeier C, Brunet JF (2011) Homeoprotein Phox2b commands a somatic-to-visceral switch in cranial sensory pathways. *Proc Natl Acad Sci USA* 108:20018–20023.
31. Monzo HJ, et al. (2012) A method for generating high-yield enriched neuronal cultures from P19 embryonal carcinoma cells. *J Neurosci Methods* 204:87–103.
32. Hernandez-Miranda LR, et al. (2017) Genetic identification of a hindbrain nucleus essential for innate vocalization. *Proc Natl Acad Sci USA* 114:8095–8100.